Title

ELECTRONIC CHARGE DENSITIES FOR ZnS IN THE WURTZITE AND ZINCBLENDE STRUCTURES

Authors

Joannopoulos, John D.
Cohen, Marvin L.

Publication Date

1972-10-01

Submitted to Physical Review

LBL-1193
Preprint

ELECTRONIC CHARGE DENSITIES FOR ZnS IN THE WURTZITE AND ZINCBLENDE STRUCTURES

John D. Joannopoulos and Marvin L. Cohen

October 1972

AEC Contract No. W-7405-eng-48

LBL-1193

DISCLAIMER

LBL-1193

Electronic Charge Densities for ZnS in the Wurtzite and Zincblende Structures

John D. Joannopoulos and Marvin L. Cohen*

Department of Physics, University of California

and

Inorganic Materials Research Division, Lawrence Berkeley Laboratory

Berkeley, California 94720

Abstract

Using the Empirical Pseudopotential Method we have calculated electronic charge densities as a function of position in the unit cell for ZnS in a zincblende and ideal wurtzite structure. A comparison of the charge densities reveals the presence of a net polarization in the ideal wurtzite structure. Two representative $\vec{k}$ points are found whose total charge density is in very good agreement with the charge density obtained by summing over many points in the irreducible part of the Brillouin zone.

I. INTRODUCTION

In a recent paper J. P. Walter and M. L. Cohen[1] reported a calculation of electronic charge densities for seven diamond and zincblende

semiconductors using the Empirical Pseudopotential Method (EPM). In particular they studied and described the various trends in bonding and ionicity for Ge, GaAs, ZnSe, α-Sn, InSb, CdTe, and Si.

In this paper we wish to compare the electronic distributions in two different crystal structures of the same compound. Thus we have calculated the electronic charge density as a function of position in the unit cell for ZnS in the wurtzite and zincblende structures. The charge density was obtained individually for each valence and conduction band and for the sum of the valence bands from a band structure calculation using the EPM. Although we do not contend that the charge densities can reveal physically accurate quantitative details since the differences between zincblende and wurtzite are so small, they can certainly provide interesting information about short and long range effects arising from the crystalline potential.

In Section II we give a description of the Empirical Pseudopotential Theory and a discussion of the validity of the wavefunctions. In Section III we proceed to discuss the calculational method used in obtaining the charge densities and in Section IV we describe and interpret the results. In Section V we give discussion of charge densities obtained from representative $\vec{k}$-points and in Section VI we make some concluding remarks.

II. PSEUDOPOTENTIAL THEORY AND WAVEFUNCTIONS

In this section we shall give a brief description of the various aspects of the Empirical Pseudopotential Theory which are relevant to our

calculation. A much more thorough and extensive treatment can be found in reference 2.

In the EPM and other one electron theories one assumes that the crystal is made up of rigid tightly bound spherical ions and a system of valence or conduction electrons. It is the latter group of electrons which are of interest since they are responsible for the physical and chemical nature of the crystal. One now separates the total one electron crystalline potential into two parts: (1) a set of spherical[3] potentials centered on the atoms which makes up the "cores", and (2) the potential everywhere else in a region outside the spheres called the interstitial region. In region (1) the potentials are strong in the sense that they have bound core and valence wavefunctions. In region (2) the potential is comparably weak and slowly varying. Thus inside the core the valence electron wavefunctions will be atomic-like with many oscillations due to the large kinetic energy caused by the deep potential well, whereas in the interstitial region the valence electron wavefunctions can be taken to be plane-wave like.

In the pseudopotential theory one begins by expanding a Bloch valence wavefunction $\psi_{v,\vec{k}}(\vec{r})$ in terms of orthogonalized plane waves (OPW)'s:[4]

$$\psi_{v,\vec{k}}(\vec{r}) = \sum_c \alpha_{\vec{k}-\vec{G}}\, \psi_{OPW,\vec{k}-\vec{G}}(\vec{r}) = \sum_{\vec{G}} \alpha_{\vec{k}-\vec{G}} [e^{i(\vec{k}-\vec{G})\cdot\vec{r}} - \sum_c \langle \psi_{c,\vec{k}}(\vec{r}) | e^{i(\vec{k}-\vec{G})\cdot\vec{r}} \rangle \psi_{c,\vec{k}}(\vec{r})] \; ; \quad (1)$$

$$\psi_{v,\vec{k}}(\vec{r}) = \varphi_{v,\vec{k}}(\vec{r}) - \sum_c \langle \psi_{c,\vec{k}}(\vec{r}) | \varphi_{v,\vec{k}}(\vec{r}) \rangle \psi_{c,\vec{k}}(\vec{r}) \quad (2)$$

where $\varphi_{\vec{k}}$ is defined from Eq. (1) and $\psi_{c,\vec{k}}$ is a tight-binding Bloch core wavefunction which is a solution of the total Hamiltonian with energy ϵ_c. If one now operates on Eq. (2) with this Hamiltonian one obtains a Schrödinger equation for $\varphi_{\vec{k}}$ in terms of an effective potential V_{eff} which has two contributions: (1) a local attractive potential due to the atoms and (2) a nonlocal repulsive potential which projects $\varphi_{\vec{k}}$ on to the core states. In most cases it is a good approximation to take repulsive potentials to be local which in turn simplifies matters considerably. This V_{eff} which is now presumably small throughout the crystal and can be considered as an empirical pseudopotential which can be described usually in terms of a small set of parameters called form factors. The pseudopotential is then obtained by fitting the form factors to experimental optical data.[5] This is called the Empirical Pseudopotential Method (EPM).[2,5] The $\varphi_{\vec{k}}$ is called a pseudowavefunction and, although Eq. (2) is now no longer valid, $\varphi_{\vec{k}}$ for all practical

purposes is taken equal to $\psi_{v,\vec{k}}$ outside the region of the core.[6] Thus the essence of the pseudopotential method is to remove the strongly negative core potential and substitute it with a much weaker potential which will give the correct valence energy eigenvalues of the crystal. At the same time removing the atomic like wiggles of the valence wavefunctions inside the core leaving the correct valence wavefunctions outside the core. Since the core is usually very small, approximately 0.2 of the nearest neighbor distance, the pseudowavefunctions should be able to provide relevant information about bonding character, symmetry, and long range interactions.

III. CALCULATIONS

In this section we shall set up the secular equation for the pseudopotential Hamiltonian and desctibe the method used in obtaining the electronic charge density. The Schrödinger equation is taken as:

$$H\varphi_{n,\vec{k}}(\vec{r}) = -\frac{\hbar^2}{2m}\vec{\nabla}^2\varphi_{n,\vec{k}}(\vec{r}) + V(\vec{r})\,\varphi_{n,\vec{k}}(\vec{r}) \qquad (3)$$

and, using Bloch's Theorem:

$$\varphi_{n,\vec{k}}(\vec{r}) = e^{i\vec{k}\cdot\vec{r}} \sum_{\vec{G}} \alpha_n(\vec{G},\vec{k}) e^{-i\vec{G}\cdot\vec{r}} \qquad (4)$$

where the set $\{\vec{G}\}$ is the set of reciprocal lattice vectors for the particular lattice in question. Usually it is only necessary to take about 90 plane waves in the expansion for $\varphi_{\vec{k}}$ to obtain good convergence for a charge density calculation.[7]

Now $V(\vec{r})$ is the total crystalline pseudopotential so that it can

be written as a sum of atomic pseudopotentials:

$$V(\vec{r}) = \sum_{\vec{R},\vec{\tau}_\lambda} T_\lambda v(\vec{r} - \vec{R} - \vec{\tau}_\lambda) \tag{5}$$

where $\vec{R}$ is a real space lattice vector, $\vec{\tau}_\lambda$ is the position of the λth atom in the primitive cell and $T_\lambda v(\vec{r}) = v_1(\vec{r})$ or $v_2(\vec{r})$, depending on whether λ denotes an atom of type 1 or type 2. Since $V(\vec{r})$ has the periodicity of the lattice we can take:

$$V(\vec{r}) = \sum_{\vec{G}} V(\vec{G}) e^{i\vec{G}\cdot\vec{r}} \tag{6}$$

and if we use Eq. (5), $V(\vec{G})$ can be expressed as:

$$V(\vec{G}) = S^S(\vec{G})\, V^S(|\vec{G}|) + iS^A(\vec{G})\, V^A(|\vec{G}|) \tag{7}$$

where S^S and S^A are the symmetric and antisymmetric structure factors and V^S and V^A are the symmetric and antisymmetric form factors given by:

$$S^S(\vec{G}) = \frac{1}{n}\sum_\lambda e^{-i\vec{G}\cdot\vec{\tau}_\lambda} \tag{8a}$$

$$S^A(\vec{G}) = -\frac{i}{n}\sum_\lambda P_\lambda e^{-i\vec{G}\cdot\vec{\tau}_\lambda} \tag{8b}$$

$$V^S(|\vec{G}|) = \frac{n}{\Omega}\int \frac{1}{2}[v_1(\vec{r}) + v_2(\vec{r})] e^{-i\vec{G}\cdot\vec{r}}\, d^3\vec{r} \tag{9a}$$

$$V^A(|\vec{G}|) = \frac{n}{\Omega}\,\frac{1}{2}[v_1(\vec{r}) - v_2(\vec{r})] e^{-i\vec{G}\cdot\vec{r}}\, d^3\vec{r} \tag{9b}$$

where n is the number of atoms in the primitive cell of volume Ω and P_λ is +1 or -1 if λ denotes an atom of type 1 or type 2. Here we have assumed that the form factors are independent of energy, and since the atomic potentials are taken to be spherical, the form factors are functions of $|\vec{G}|$ only. If in addition we place the center of our coordinate system in such a way that the atoms of type 1 interchange their positions with atoms of type 2 under spacial inversion, then S^S and S^A are both real. The secular equation is now easily obtained from (3) using (4), (6) and (3) and has the form:

$$\left| H_{\vec{G},\vec{G}'}(\vec{k}) - E_n(\vec{k})\,\delta_{\vec{G}\vec{G}'} \right| = 0 \qquad (10)$$

where

$$H_{\vec{G}\vec{G}'}(\vec{k}) = \frac{\hbar^2}{2m}(\vec{k}+\vec{G})^2\delta_{\vec{G}\vec{G}'} + V^S(|\vec{G}-\vec{G}'|)S^S(\vec{G}-\vec{G}') +$$

$$+ iV^A(|\vec{G}-\vec{G}'|)\,S^A(\vec{G}-\vec{G}') \quad . \qquad (17)$$

In order to obtain good convergence in the calculation of energy eigenvalues and dipole matrix elements, it is usually[8] adequate to diagonalize only a 25 x 25 matrix where 25 plane waves are taken directly into account and the effect of 80 more plane waves is brought in through the use of a perturbation technique due to Löwdin.[9]

In reference 5 it is shown that for a zincblende crystal it is only necessary to consider six form factors in the

expansion of $V(\vec{r})$. The reason for this is that the form factors become very small after a certain cutoff $|\vec{G}_0|$ and higher $V(\vec{G})$ can be accounted for through variations in form factors with lower $\vec{G}$'s. Therefore $V(\vec{G})$ for $|\vec{G}| > |\vec{G}_0|$ can be neglected. For the cubic case one can take[10] $|\vec{G}_0|^2 = 16$ which leaves five possible $|\vec{G}|$'s in the range $0 < |\vec{G}| < |\vec{G}_0|$. However, for some of these $|\vec{G}|$'s the structure factors are zero so that one is finally left with just three symmetric and three antisymmetric form factors as parameters.

In the hexagonal case one has fifteen $|\vec{G}|$'s in the range $0 < |\vec{G}| < |\vec{G}_0|$ and if one considers the effect of the structure factors one would be left with ten symmetric and nine antisymmetric form factors. However instead of varying nineteen parameters Bergstresser and Cohen[11] used the form factors from the cubic case and interpolated to obtain the form factors of the hexagonal case. This method was able to account well for the optical spectra of three hexagonal crystals and it is these form factors that we used in our study of ZnS.

The two crystal structures are shown in Fig. 1, with the wurtzite structure aligning so that the c axis is in the z direction and the zincblende structure is aligned with its (1 1 1) direction in the z direction. The difference between the two structures occurs first at third nearest neighbors.

All the crystal parameters used in our calculation were obtained from Wycoff.[12] In the zincblende case one only needs the lattice constant a_c to specify the size of the structure; for ZnS we take $a_c = 5.41$ Å. In the wurtzite case, however, one needs three parameters: $a_h = 3.811$ Å, $c_h = 6.223$ Å and $u = 0.375$. The values for c_h and u are for a

an ideal structure, i.e. perfect tetrahedral coordination.

We now have in principle all the information necessary to obtain the charge density. Since the wavefunctions are known as a function of band index we can postulate a "band" charge density:

$$\rho_n(\vec{r}) = e \sum_{n}^{BZ} \varphi^*_{n,\vec{k}}(\vec{r})\, \varphi_{n,\vec{k}}(\vec{r}) \qquad (11)$$

$$\rho_n(\vec{r}) = e \sum_{\vec{\Gamma}} \sum_{\vec{G}} \sum_{\vec{k}}^{B.Z.} \alpha^*_n(\vec{G}-\vec{\Gamma},\vec{k})\, \alpha_n(\vec{G},\vec{k}) \,. \qquad (12)$$

The total charge density is then given by

$$\rho(\vec{r}) = \sum_{n} \rho_n(\vec{r}) \qquad (13)$$

where the sum in (13) is over the valence bands.

The expression in Eq. (12) is a general result; however, the procedure involved in evaluating this expression depends on the symmetry properties of the crystal studied. The zincblende charge density calculation was carried out exactly as in reference 1. The wurtzite charge density calculation will now be described in some detail.

The Brillouin Zone (BZ) for the hexagonal structure and its irreducible part are well known. Although the energies $E_n(\vec{k})$ are exactly the same at related points in the BZ, the wavefunctions in general are not. Our procedure was to calculate the $\varphi_{n,\vec{k}}$ in one twenty-fourth of the zone at 48 points and obtain the rest of the $\varphi_{n,\vec{k}}$ by rotations of $\pi/3$, inversions

and mirror reflections in k space. In order to find how the $\varphi_{n,\vec{k}}$ transform one must go back to real space and study the symmetry operations of the crystal. Since the wurtzite crystal has a symmetry classification of $P6_3mc$, any rotations of $\pi/3$ in real space, must be accompanied by certain translations. Once the space group elements are found, the procedure to find the transformed wavefunctions is now simple. Let us assume that R^{-1} is some rotation in the point group in the negative sense. In order to make U a symmetry operator of the wurtzite crystal we must take generally:

$$U = TR^{-1} \tag{14}$$

where T is the appropriate translation operator with eigenvalue $\vec{t}_R$. Now $\varphi_{n,\vec{k}}(\vec{r})$ has the form:

$$\varphi_{n,\vec{k}}(\vec{r}) = e^{i\vec{k}\cdot\vec{r}} \sum_{\vec{G}} \alpha_n(\vec{G},\vec{k}) e^{i\vec{G}\cdot\vec{r}} . \tag{15}$$

However

$$\varphi_{n,\vec{k}}(U\vec{r}) = e^{i\vec{k}\cdot U\vec{r}} \sum_{\vec{G}} \alpha_n(\vec{G},\vec{k}) e^{i\vec{G}\cdot U\vec{r}} \tag{16}$$

is also a solution to H with exactly the same eigenvalue as $\varphi_{n,\vec{k}}(\vec{r})$. Thus we wish to find $\vec{k}'$ such that:

$$\varphi_{n,\vec{k}'}(\vec{r}) = \varphi_{n,\vec{k}}(U\vec{r}) . \tag{17}$$

From (14) and (16) we have:

$$\varphi_{n,\vec{k}}(U\vec{r}) = e^{i\vec{k}\cdot R^{-1}\vec{r}} e^{i\vec{k}\cdot\vec{\tau}_R} \sum_{\vec{G}} \alpha_n(\vec{G},\vec{k}) e^{i\vec{G}\cdot R^{-1}\vec{r}} e^{i\vec{G}\cdot\vec{\tau}_R} \quad (18)$$

$$\varphi_{n,\vec{k}}(U\vec{r}) = e^{iR\vec{k}\cdot\vec{r}} e^{i\vec{k}\cdot\vec{\tau}_R} \sum_{\vec{G}} \alpha_n(R^{-1}\vec{G},\vec{k}) e^{i\vec{G}\cdot\vec{r}} e^{iR^{-1}\vec{G}\cdot\vec{\tau}_R} \quad (19)$$

and Eq. (19) follows from the fact that the set $\{\vec{G}\}$ is equal to the set $\{R^{-1},\vec{G}\}$. Now since

$$\varphi_{n,\vec{k}'}(\vec{r}) = e^{i\vec{k}'\cdot\vec{r}} \sum_{\vec{G}} \alpha_n(\vec{G},\vec{k}') e^{i\vec{G}\cdot\vec{r}} \quad (20)$$

a comparison of (20) with (19) reveals that if we let $\vec{k}' = R\vec{k}$ we obtain:

$$\alpha_n(\vec{G},R\vec{k}) = e^{i\vec{k}\cdot\vec{\tau}_R} \alpha_n(R^{-1}\vec{G},\vec{k})\, e^{iR^{-1}\vec{G}\cdot\vec{\tau}_R} \quad (21)$$

which is the required transformation expression.

To obtain a transformation expression involving the inversion operation we must use the concept of the reversal symmetry. Thus we look at

$$\varphi^*_{n,\vec{k}}(\vec{r}) = e^{i\vec{k}\cdot\vec{r}} \sum_{\vec{G}} \alpha^*_n(\vec{G},\vec{k}) e^{-i\vec{G}\cdot\vec{r}} \quad . \quad (22)$$

If we now compare (20) and (23) and take $\vec{k}' = I\vec{k} = -\vec{k}$ we obtain:

$$\alpha_n(\vec{G},-\vec{k}) = \alpha^*_n(-\vec{G},\vec{k}) \quad (23)$$

which is the desired expression.

Finally we need to find the transformation expression for the mirror reflection operator. If we choose the mirror plane to be the plane defined

by Γ, M and A then we will have all the transformations necessary to span all of k space inside the Brillouin zone. In real space this mirror plane becomes plane I shown in Fig. 1. It is clear that this mirror operator M is by itself a symmetry operator of the crystal. Thus proceeding as before:

$$\varphi_{n,\vec{k}}(M\vec{r}) = e^{i\vec{k}\cdot M\vec{r}} \sum_{\vec{G}} \alpha_n(\vec{G},\vec{k}) e^{i\vec{G}\cdot M\vec{r}} \quad ; \tag{24}$$

$$\varphi_{n,\vec{k}}(M\vec{r}) = e^{iM\vec{k}\cdot\vec{r}} \sum_{\vec{G}} \alpha_n(M\vec{G},\vec{k}) e^{i\vec{G}\cdot\vec{r}} \quad . \tag{25}$$

From this it follows that:

$$\alpha_n(\vec{G},M\vec{k}) = \alpha_n(M\vec{G},\vec{k}) \tag{26}$$

and we now have all the transformations equations needed to obtain the wavefunctions throughout the Brillouin zone.

IV. RESULTS

It would be appropriate at this point to say something more quantitative about the size of the Zn and S cores. The electronic configuration of the Zn and S cores is $1s^2 2s^2 2p^6 3s^2 3p^6 3d^{10}$ and $1s^2 2s^2 2p^6$ respectively. Using the wavefunctions obtained by Herman and Skillman[2] we found that:

(i) 90% of all the Zn core electrons are within a radius of 12% of the

nearest neighbor distance. In particular this radius contains 86% of the 3d shell, 93% of the 3p and 3s shells and approximately 100% of the rest.

(ii) 90% of all the S core electrons are within a radius of 0.16 of the nearest neighbor distance. In particular this radius contains approximately 88% of the 2p and 2s shells and approximately 100% of the 1s shell.

We are confident that for such small cores the wavefunctions are quite adequate.

A. Cubic.

In the cubic case, chains of bonds that lie in a plane only occur in a zig-zag pattern. If one sights along the direction of any bond one sees the same symmetrical distribution or environment of atoms. Thus the effects of this environment through long range electrostatic interactions will be along the direction of the bonds and the short range tetrahedral symmetry will be preserved.

We found the charge density of ZnS in the zincblende structure to be very similar to that of ZnSe obtained by Walter and Cohen.[1] Because of this similarity we show in Fig. 2 only a contour plot of the total charge density. There is only one type of plane of interest and that is the $(1\bar{1}\ 0)$ plane or the plane formed by the dotted lines in Fig. 1b. The charge density was evaluated on a grid of over 1500 points. In Fig. 3 we show a contour plot of the total crystalline pseudopotential, obtained from (6), in the same plane as the charge density. The potential was evaluated on

a grid of over 3500 points and the zero of potential was chosen arbitrarily such that the average crystalline potential is zero. The tetrahedral symmetry in Figs. 2 and 3 is evident. The amount of charge around the S atom within a radius of 3/4 the nearest neighbor distance is approximately 7.3 e, and only 2% of this charge is in the core region.

B. Hexagonal.

In the wurtzite structure we have four atoms in the unit cell so that we have eight valence bands. We found that the charge density of bands 1 and 2 are almost identical so that in Figs. 4, 5, 6, and 7 we show contour plots of the charge density for bands 1, 3, 4, 5, 6, 7 and 8. In Fig. 7 we also show a plot for the hypothetical situation where the conduction band is full of electrons. The plane in these figures is the (1 1 0) plane or plane I in Fig. 1a. The charge densities were evaluated on a grid of more than 4000 points. We notice that bands 1 and 2 are very s-like whereas the rest of the bands have pronounced p-like character. In particular bands 6 and 8 are almost pure p_{xy}-like and p_z-like respectively. We also notice that the character of the conduction band is almost free electron-like although there still is some localization around the S atoms. In Fig. 8 we show a plot of the total charge density in plane I. In this plane the atoms form square wave-like chains of bonds which cannot be found in zincblende. The zig-zag patterns in the cubic case, however, can be found in the (1 0 1) plane or plane II in Fig. 1a. A contour plot of the total charge density in this plane is

shown in Fig. 9. In Figs. 10 and 11 we also show contour plots of the total charge density in planes III and IV. These planes help provide a three-dimensional view of the charge density. Comparing Figs. 8 and 9 we notice immediately an assymmetry in the electron distribution. Although the ionic cores are in a perfect tetrahedral arrangement the charge density is not. There seems to be a difference between bonds in the z directions and bonds in the other three corresponding tetrahedral directions. Firstly the maximum charge density occurs only for bonds in the z direction and secondly the charge density is pushed slightly out of the bond for those bonds which are not in the z direction. This asymmetry is actually a direct manifestation of the potential. This is clear in Fig. 12 in which we show contour plots of the crystalline pseudopotential in plane I.

Actually these results are not surprising. In the zincblende structure the environment of each bond is the same for all bonds. In the wurtzite structure, however, this is not the case. If one sights along a bond in the z direction all the atoms which affect it are placed symmetrically, in planes perpendicular to the z direction. The net effect of these atoms is then directed along the bond. If one now sights along any other bond not in the z direction one finds an asymmetrical distribution of atoms. The net effect of this type of environment is not directed along the bond, but actually directed slightly out of the bond. To show this in a simple way consider the following model. We assume we can construct a ZnS crystal

out of two types of constituents: (1) positively charged Zn cores with a charge of $2e^-$ and (2) S cores surrounded by a perfect tetrahedral distribution of electrons as in Fig. 2 of the cubic charge density. The net charge on this second part being $-2e^-$. We are thus taking implicitly into account the short range interactions and we shall be interested in the effect of long-range electrostatic interactions on the bond electrons of type (2) constituents. If we now arrange these constituents in a zinc-blende structure and calculate the net electric field acting on these electrons we find of course that the field is directed along the bond preserving the tetrahedral symmetry. However, if we construct a wurtzite crystal out of these constituents and calculate the net electric field on the electrons in the diagonal bonds we find that the field is directed primarily along the bond direction apart from a small z component which has the effect of pushing electrons out of the bond in the positive z direction. This is exactly what we find in our charge densities.

This asymmetrical distribution of charge in "ideal" wurtzite will produce a polarization. We can calculate the dipole moment p per primitive cell analytically using the fourier expansion of the charge density. We find:

$$p \sim 10^{-19} \text{ esu cm} . \qquad (27)$$

This is only about 50 times smaller than a usual ferroelectric-like $BaTiO_3$. Although we do not expect our value for p to be accurate we do believe that there will be a resultant polarization. This polarization

will then change the electronic and core positions so that the crystal reaches a lower energy state and the polarization is minimized. This tempts one to suggest that the non-ideal c/a ratio found in real crystals results from changes in the crystal structure to reduce p. We are in the process of further investigations alone these lines.

VI. REPRESENTATIVE k VECTORS FOR TOTAL CHARGE DENSITY

The idea here is to find a few $\vec{k}$ points whose charge density will give a good approximation to the total charge density. Baldereschi[14] first proposed this and obtained one representative $\vec{k}$ point which gave an approximate total charge density for compounds in an fcc lattice. Chadi and Cohen[15], using wavefunctions expanded in terms of Wannier functions, obtained three representative $\vec{k}$ points at whose weighted sum of charge densities gives better agreement than the Baldereschi point.

In this section we wish to present a simple method of obtaining the same conditions for the k points without using any wavefunctions. Let $\hat{\rho}(\vec{r})$ be defined in the following way:

$$\hat{\rho}(\vec{k},\vec{r}) = \sum_{T} \rho(T\vec{k},\vec{r}) \tag{28}$$

where $\rho(\vec{k},\vec{r})$ is the charge density of the point $\vec{k}$ and $\{T\}$ represents the set of point operations for the point $\vec{k}$. Now $\hat{\rho}_{\vec{k}}(\vec{r})$ is a periodic function of $\vec{k}$, so that we can expand it in the following way:

$$\hat{\rho}(\vec{k},\vec{r}) = \sum_{\vec{\ell}} \hat{\rho}(\vec{\ell},\vec{r}) e^{i\vec{k}\cdot\vec{\ell}} \quad . \tag{29}$$

Now since $\hat{\rho}(\vec{k},\vec{r}) = \hat{\rho}(T\vec{k},\vec{r})$, $\hat{\rho}(\vec{\ell},\vec{r}) = \hat{\rho}(T\vec{\ell},\vec{r})$. Therefore

$$\hat{\rho}(\vec{k},\vec{r}) = \sum_{\vec{\ell}} \hat{\rho}(\vec{\ell},\vec{r}) \sum_{T} e^{i\vec{k}\cdot T\vec{\ell}} \tag{30}$$

$$\hat{\rho}(\vec{k},\vec{r}) = \sum_{\vec{\ell}} \hat{\rho}(\vec{\ell},\vec{r})\, \xi(\vec{k},\vec{\ell}) \tag{31}$$

where $\hat{\rho}(0,\vec{r})$ is the total charge density in question. Thus if we could find a $\vec{k}_0$ that makes all the $\xi(\vec{k},\vec{\ell})$ equal to zero for $\vec{\ell} \neq 0$ then $\hat{\rho}(\vec{k}_0,\vec{r})$ would be exactly equal to the total charge density. We have found that $\rho(\vec{k},\vec{r})$ is a slowly varying function of $\vec{k}$ so that we expect the $\hat{\rho}(\vec{\ell},\vec{r})$ to decrease in magnitude as $|\vec{\ell}|$ increases. The object then is to find a $\vec{k}_0$ which will make as many of the $\xi(\vec{k}_0,\vec{\ell})$ for small $|\vec{\ell}|$ equal to zero as possible. The Baldereschi point gives ξ equal to zero for the first two $|\vec{\ell}|$ shells. The Chadi and Cohen scheme gives ξ for the first seven shells equal to zero. In this calculation we obtained two $\vec{k}$ points for an hcp lattice which give ξ equal to zero for the first ten shells except for the fifth shell. The total charge density we obtained using the average charge density of these points, agrees very well with this calculation.

The points are given by:

$$k_1 = \left(\frac{\sqrt{3}}{4}, \frac{\sqrt{3}}{8}, \frac{1}{4}\right) \tag{32}$$

$$k_2 = \left(\frac{\sqrt{3}}{8}, \frac{-\sqrt{3}}{8}, \frac{1}{4}\right) \tag{33}$$

and the components are with respect to the primitive reciprocal lattice vectors $\vec{A}$, $\vec{B}$, $\vec{C}$ for hexagonal with $\hat{A}\cdot\hat{B} = 0.5$.

VII. SUMMARY AND CONCLUSIONS

We have obtained the charge densities for ZnS in the zincblende and ideal wurtzite structures by summing over 48 points in the irreducible part of the Brillouin zone. We have found that we can obtain very good

agreement with our calculation for the wurtzite total charge density (which used many $\vec{k}$ points) if we only use two $\vec{k}$ points $\left(\frac{\sqrt{3}}{4}, \frac{\sqrt{3}}{8}, \frac{1}{4}\right)$ and $\left(\frac{\sqrt{3}}{8}, -\frac{\sqrt{3}}{8}, \frac{1}{4}\right)$.

The charge density for ZnS in the zincblende structure was, as expected, very similar to that of ZnSe. In the ideal wurtzite case we found that we have a net polarization. This was shown to be reasonable and cannot be restricted by symmetry arguments. The effect of this polarization will be to displace the electrons and cores from the ideal configuration to a configuration with less energy and a minimum polarization. It is therefore tempting to suggest that this may be the reason why no known wurtzite crystals have been found to exist with an ideal c/a and u.

Acknowledgement

Part of this work was done under the auspices of the U. S. Atomic Energy Commission.

REFERENCES

*Supported in part by National Science Foundation Grant GH 35688.

1. J. P. Walter and M. L. Cohen, Phys. Rev. B4, 1877 (1971).

2. M. L. Cohen and V. Heine, Solid State Physics 24, 37 (1970).

3. It is not necessary to have a spherical potential in the EPM although it is more convenient.

4. An O.P.W. is a plane wave minus a sum of core states such that the O.P.W is orthogonal to the core states. Thus a reasonable approximation to valence like states.

5. M. L. Cohen and T. K. Bergstresser, Phys. Rev. 141, 789 (1966).

6. J. P. Walter and M. L. Cohen have found that the pseudopotential wavefunctions agree very nicely with those of O.P.W. calculations in the regions away from the cores for the cases studied (private communication).

7. This is true in the cubic case. For the hexagonal case one needs about 135 plane waves for adequate convergence.

8. This is true for zincblende crystals. In wurtzite one needs approximately 65 plane waves.

9. P. Löwdin, J. Chem. Phys. 19, 1396 (1951).

10. In units of $(2\pi/a)^2$ where a the cubic unit cell length.

11. T. K. Bergstresser and M. L. Cohen, Phys. Rev. 164, 1069 (1967).

12. R. W. G. Wycoff, Crystal structures, vol. 1,(John Wiley & Sons, New York, 1963).

13. F. Herman and S. Skillman, Atomic structure,(Prentice-Hall, New Jersey, 1966).

14. A. Baldereschi, Bull. A. P. S. 17, 237 (1972).

15. D. J. Chadi and M. L. Cohen, Phys. Rev. in press.

FIGURE CAPTIONS

Fig. 1. (a) Wurtzite and (b) zincblende crystal structures. The wurtzite structure is aligned with the c axis along the z direction and zincblende is oriented with the (1 1 1) direction pointing along the z direction.

Fig. 2. Total charge density for ZnS in zincblende structure, (1 $\bar{1}$ 0) plane.

Fig. 3. Crystalline pseudopotential for ZnS in zincblende structure, (1 $\bar{1}$ 0) plane.

Fig. 4. ZnS wurtzite charge density - bands 1 and 3, (1 1 0) plane.

Fig. 5. ZnS wurtzite charge density - bands 4 and 5, (11 0) plane.

Fig. 6. ZnS wurtzite charge density - bands 6 and 7, (1 1 0) plane.

Fig. 7. ZnS wurtzite charge density - bands 8 and 9, (1 1 0) plane.

Fig. 8. ZnS wurtzite total charge density in plane I, (1 1 0) plane .

Fig. 9. ZnS wurtzite total charge density in plane II, (1 0 1) plane.

Fig. 10. ZnS wurtzite total charge density in plane III, (0 0 1) plane. Only the S atoms lie in this plane.

Fig. 11. ZnS wurtzite total charge density in plane IV, (1 0 0) plane. Only the S and Zn atoms in the center of the figure lie in this plane.

Fig. 12. Crystalline pseudopotential for ZnS in wurtzite structure in plane I, (1 1 0) plane.

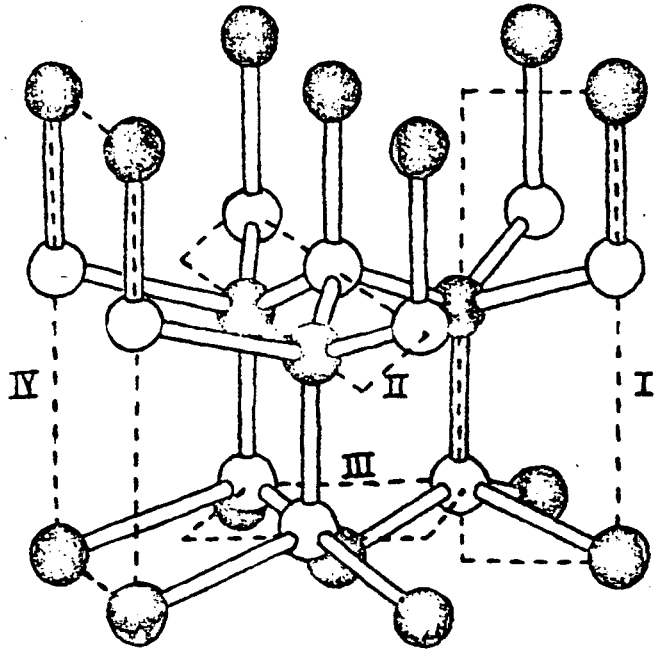

WURZITE

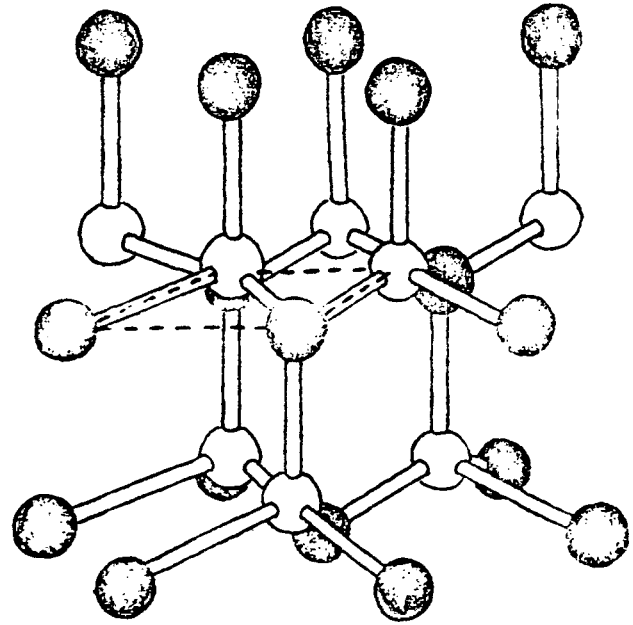

ZINC BLENDE

XBL 7211-7201

Fig. 1.

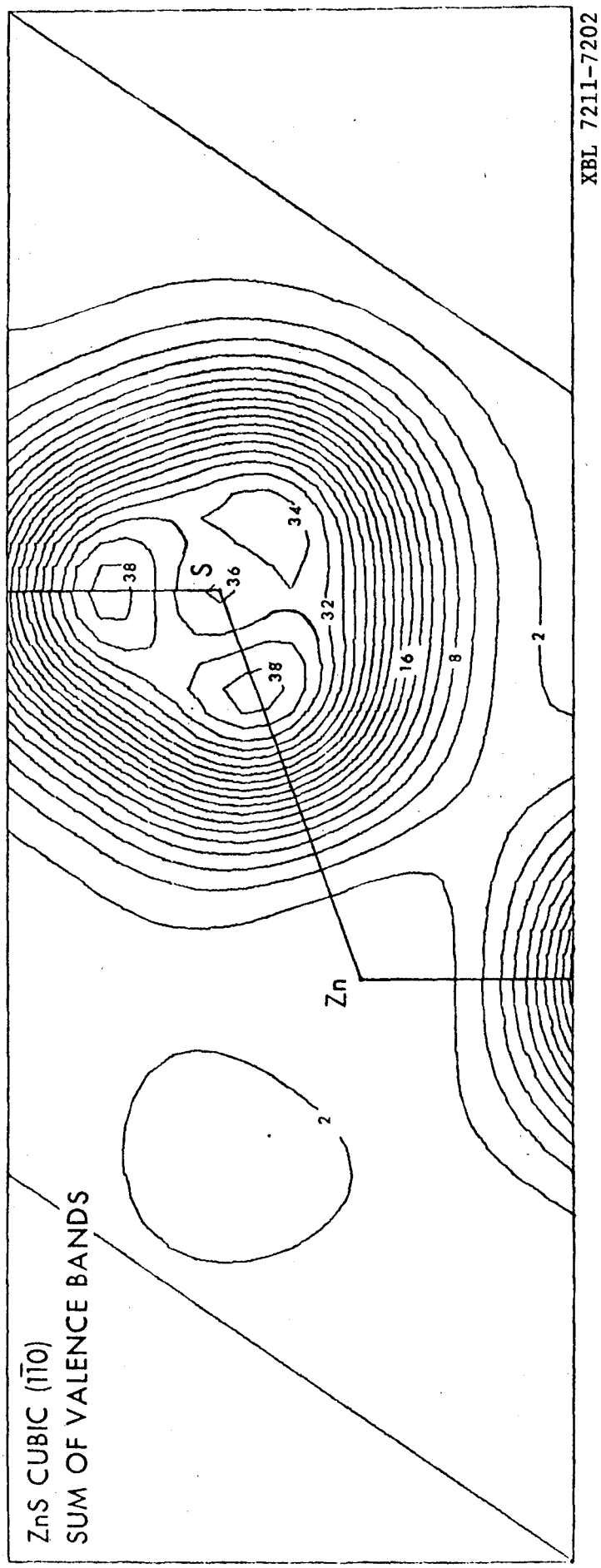
ZnS CUBIC (1$\bar{1}$0)
SUM OF VALENCE BANDS
XBL 7211-7202
S
Zn
38
36
34
32
38
16
8
2
2

Fig. 2.

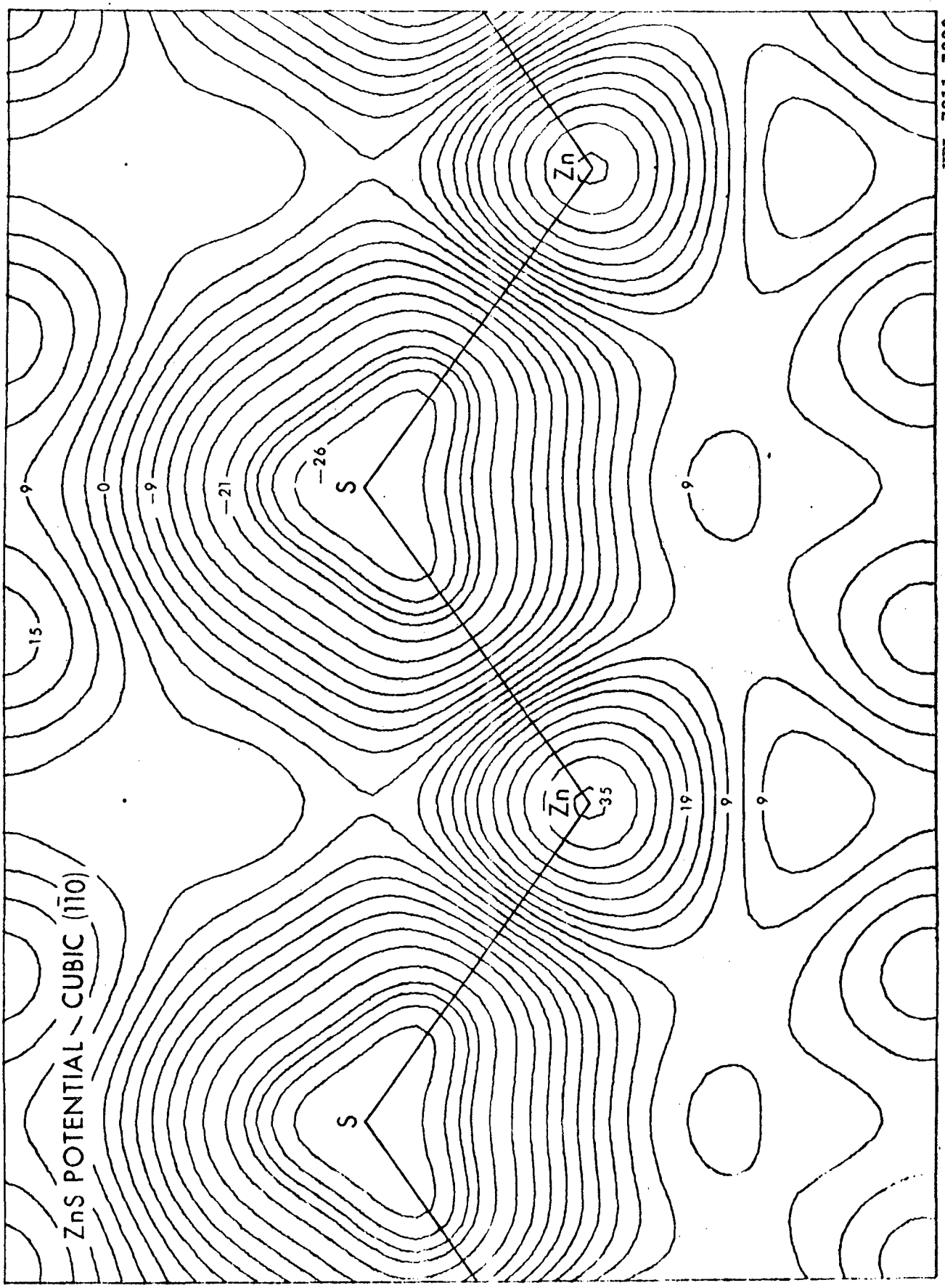
ZnS POTENTIAL — CUBIC (1$\bar{1}$0)
S
Zn
S
Zn
15
9
0
-9
-21
-26
35
19
9
9
9
XBL 7211-7203

Fig. 3.

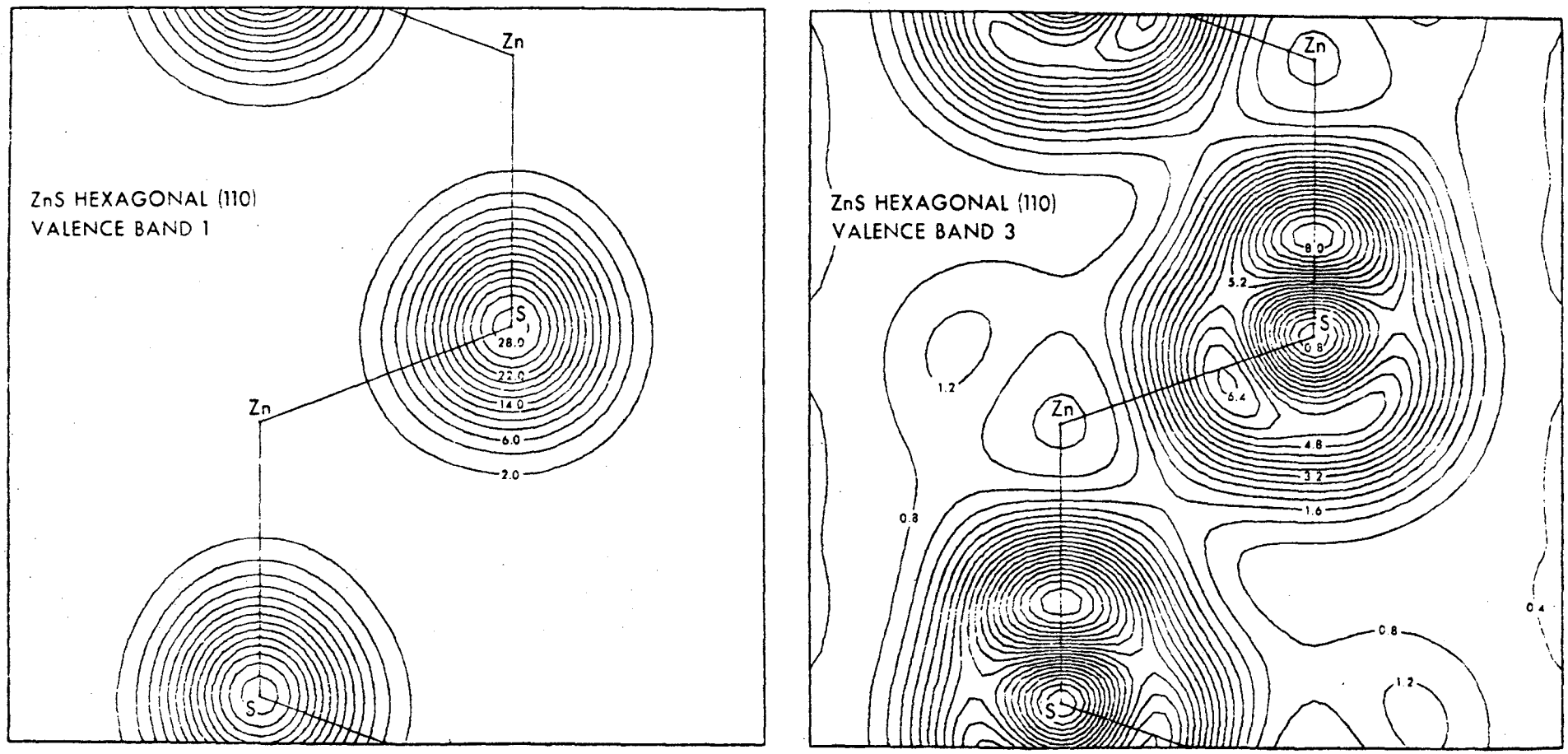

XBL 7211-7204

Fig. 4.

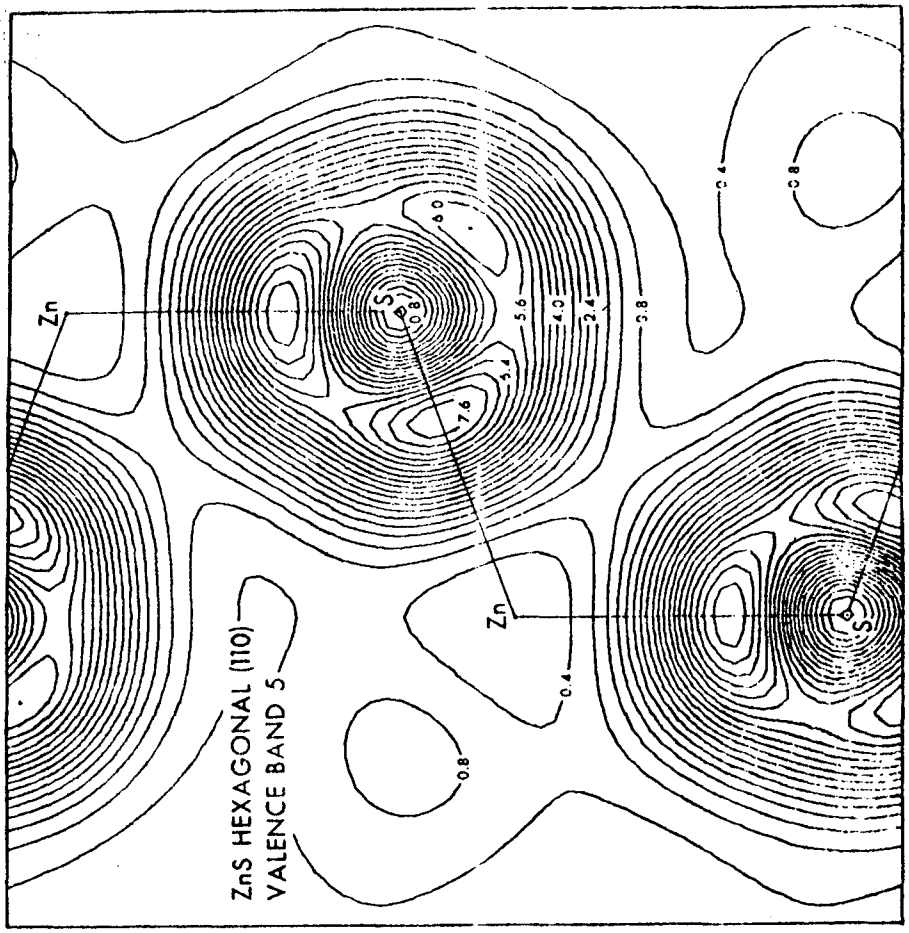

XBL 7211-7205

Fig. 5.

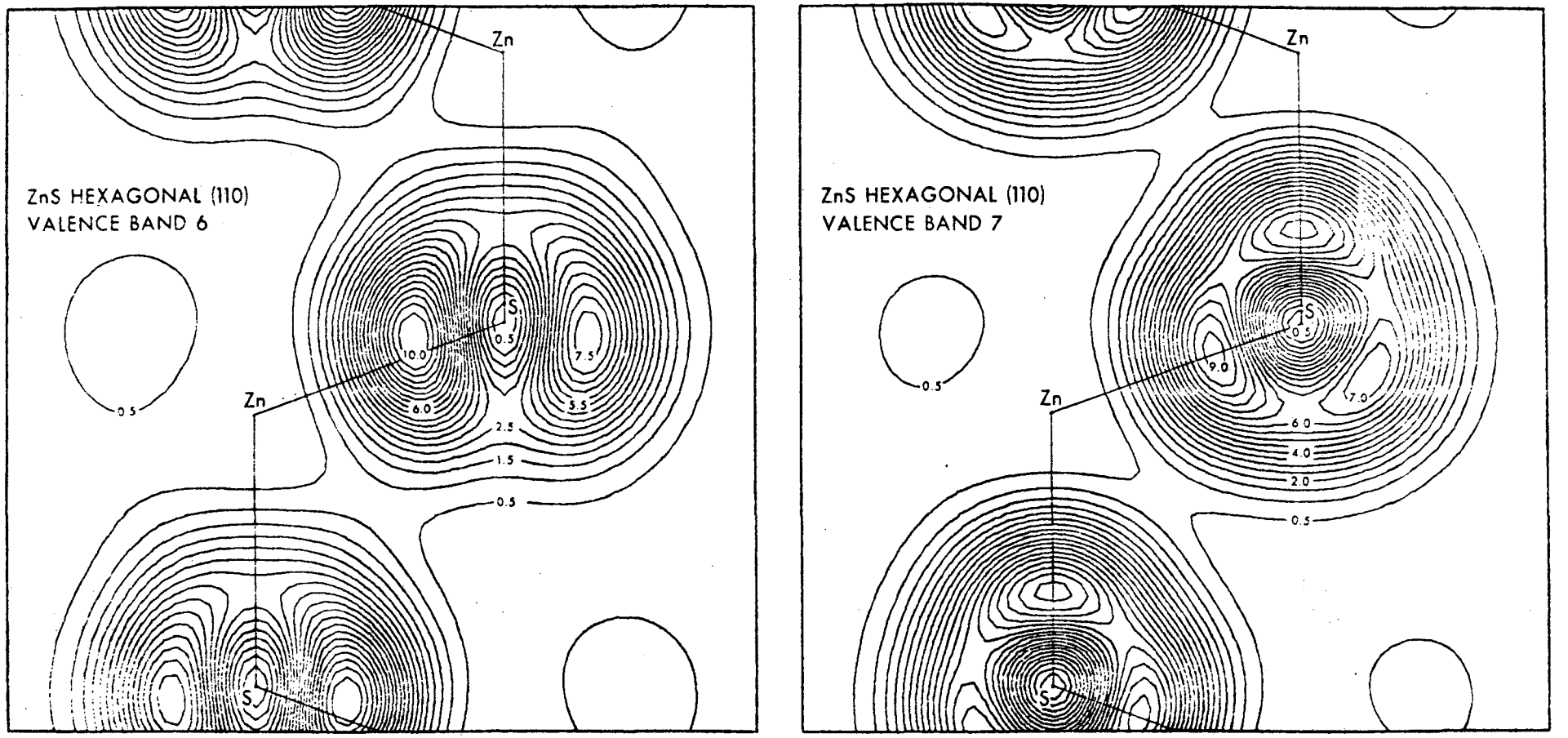

XBL 7211-7206

Fig. 6.

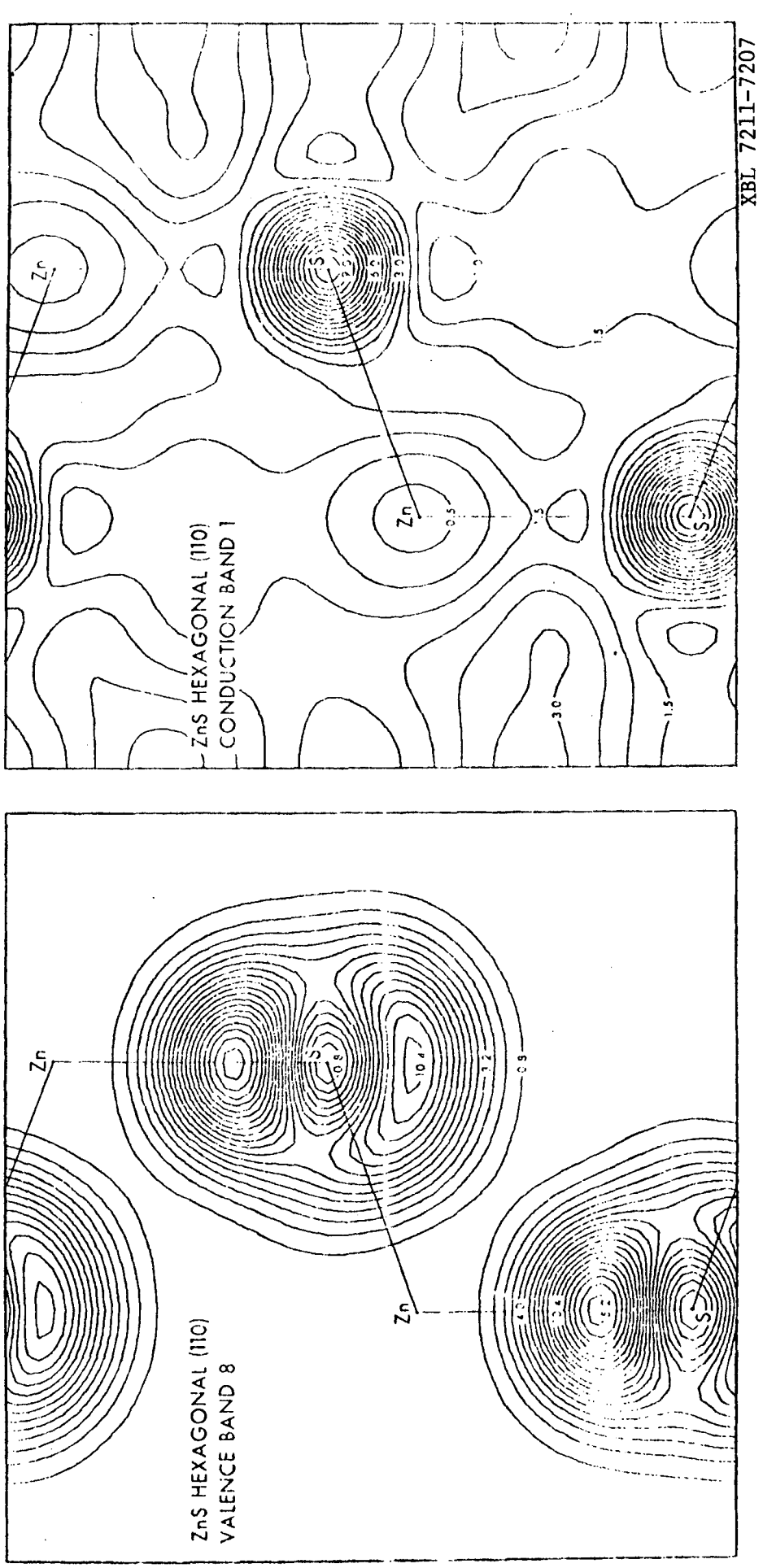
ZnS HEXAGONAL (110)
CONDUCTION BAND 1
Zn
S
Zn
S
1.5
3.0
0.5
ZnS HEXAGONAL (110)
VALENCE BAND 8
Zn
S
Zn
S
0.8
1.0
1.2
0.9
XBL 7211-7207

Fig. 7.

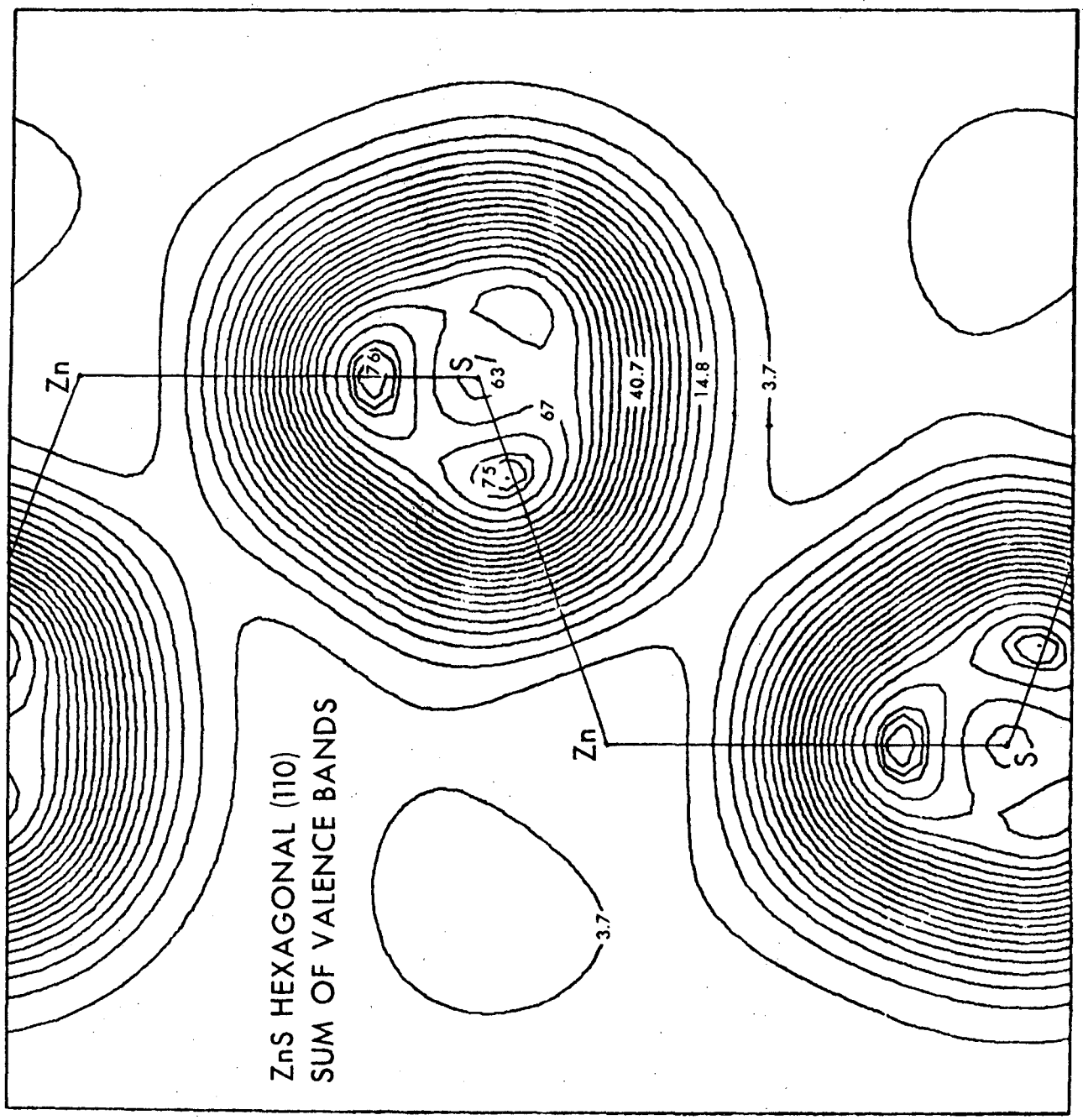

XBL 7211-7208

Fig. 8.

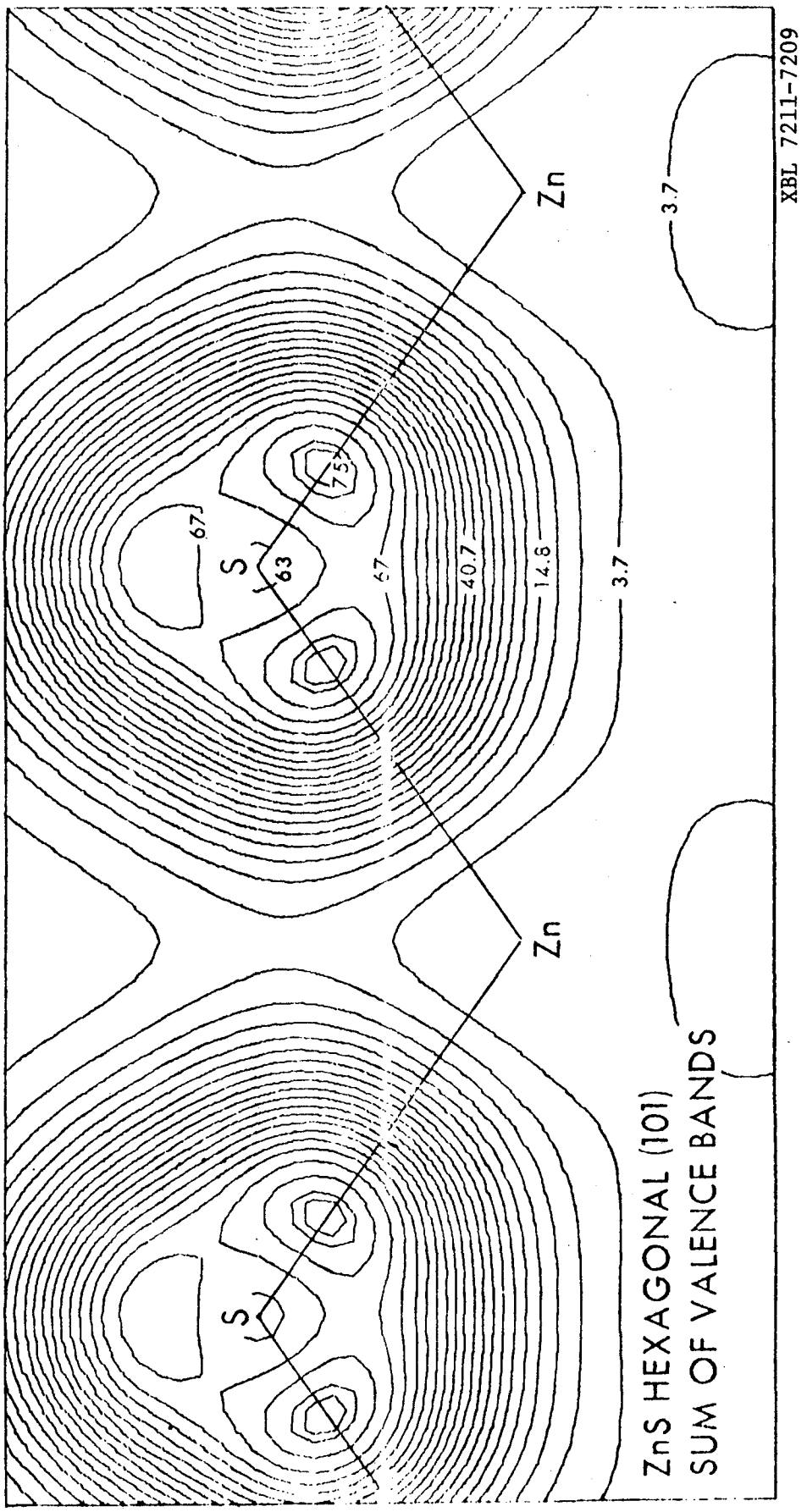
ZnS HEXAGONAL (101)
SUM OF VALENCE BANDS
Zn
Zn
S
S
67
63
75
67
40.7
14.8
3.7
3.7
XBL 7211-7209

Fig. 9.

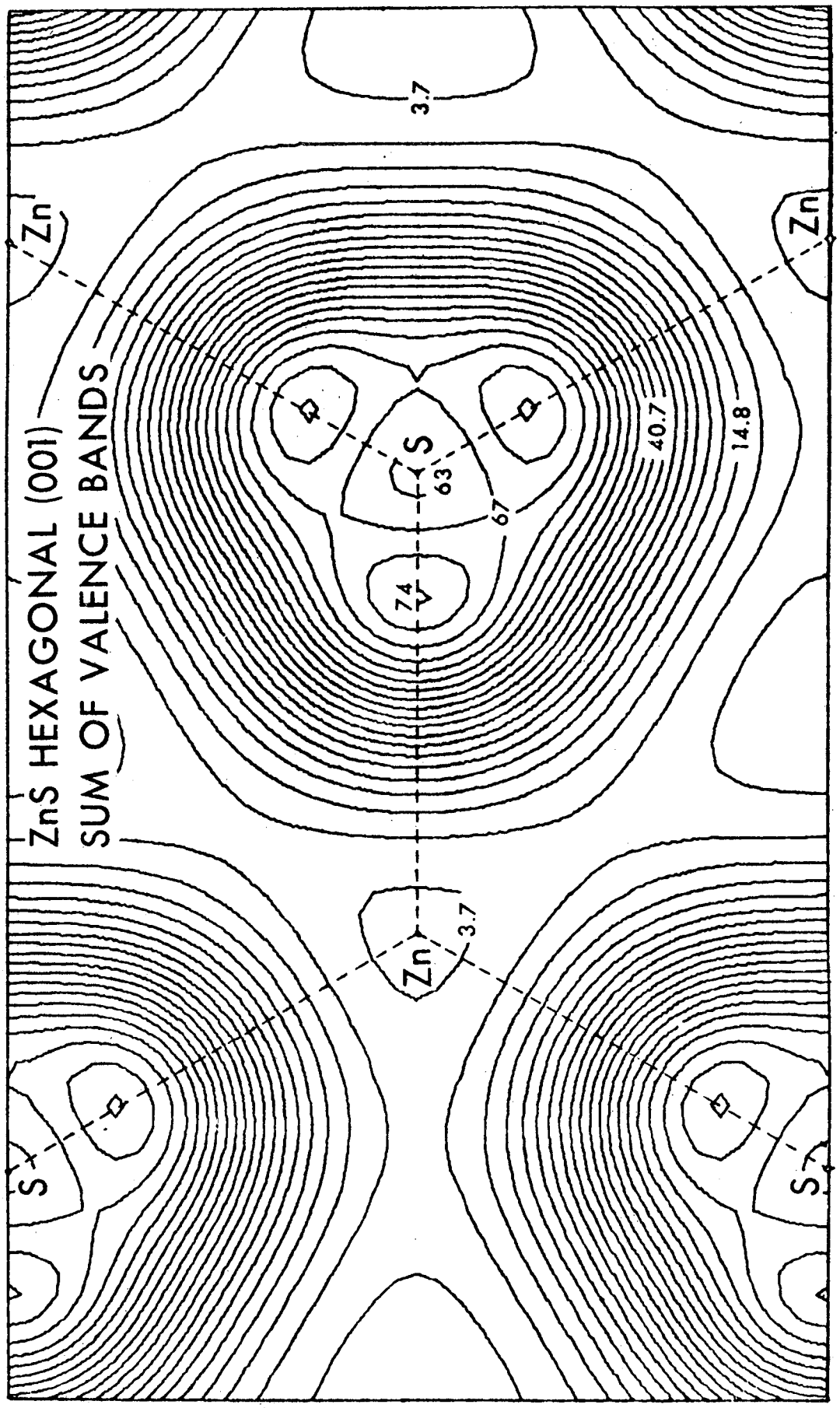

XBL 7211-7210

Fig. 10.

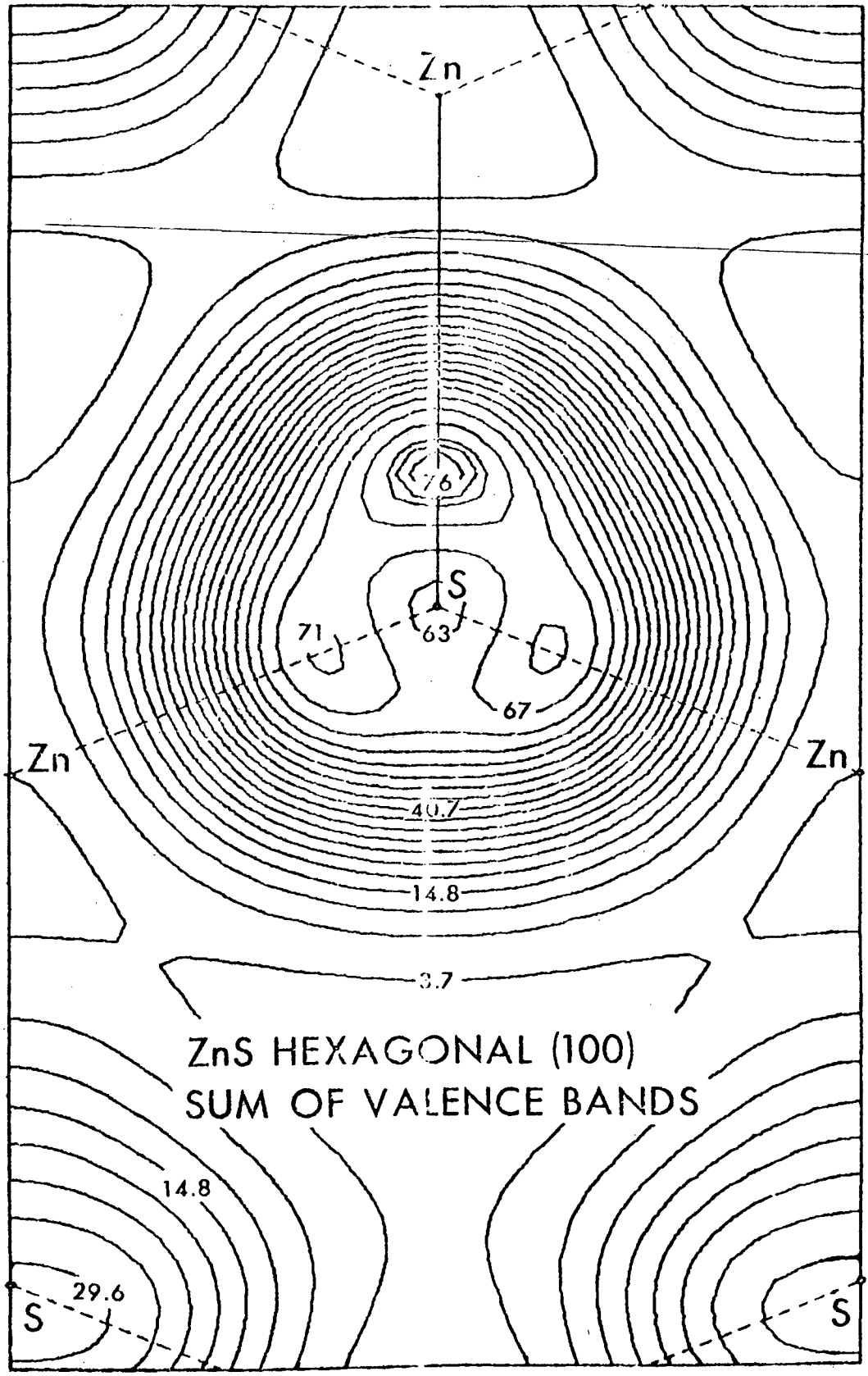

XBL 7211-7211

Fig. 11.

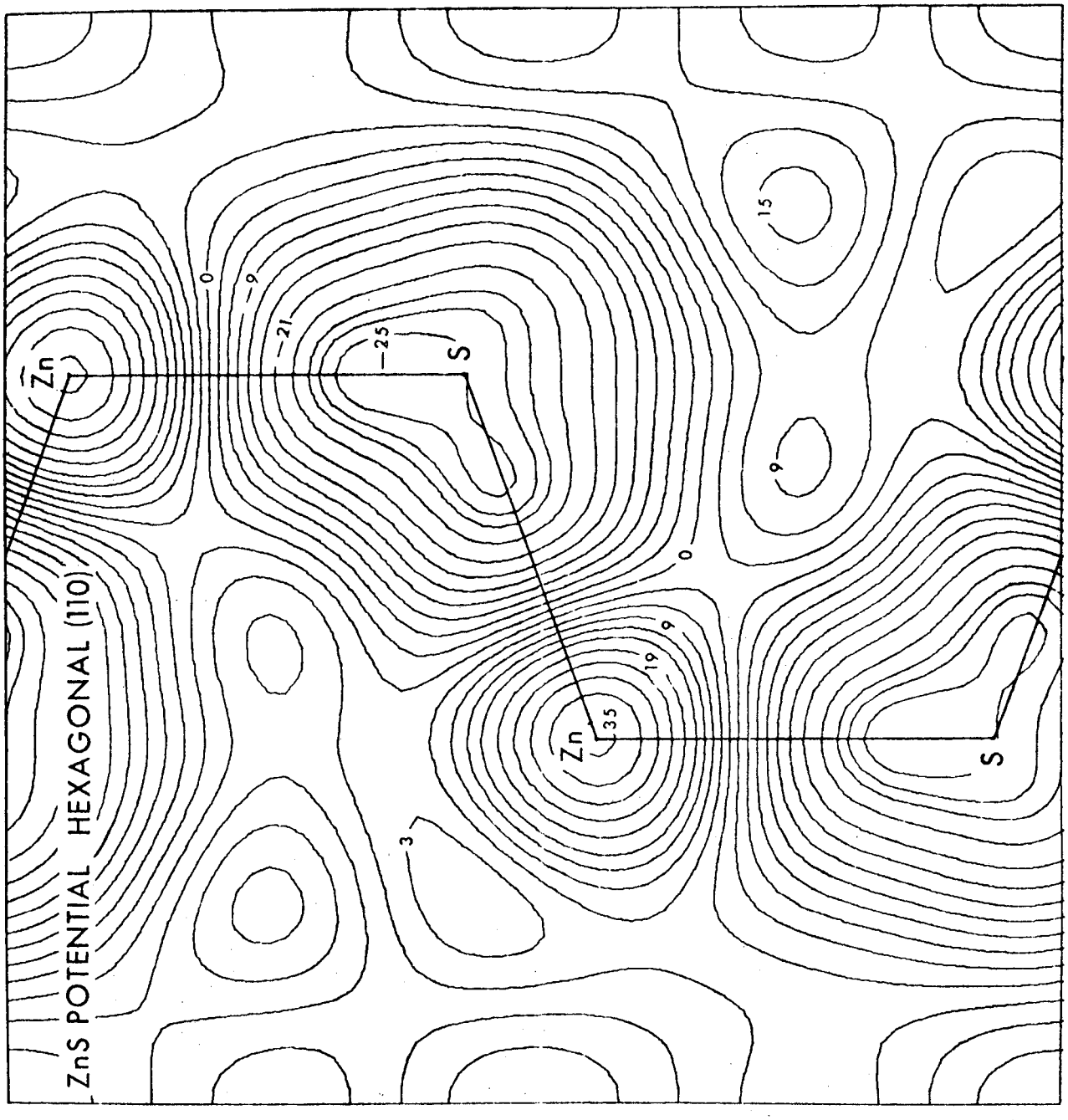
ZnS POTENTIAL HEXAGONAL (110)
Zn
S
Zn
S
0
-9
-21
-25
15
9
0
9
19
35
3
XBL 7211-7212

Fig. 12.

TECHNICAL INFORMATION DIVISION
LAWRENCE BERKELEY LABORATORY
UNIVERSITY OF CALIFORNIA
BERKELEY, CALIFORNIA 94720